Title: Re-annotation of the *Theileria parva* genome refines 53% of the proteome and uncovers essential components of N-glycosylation, a conserved pathway in many organisms

Kyle Tretina[1], Roger Pelle[2], Joshua Orvis[1], Hanzel T. Gotia[1], Olukemi O. Ifeonu[1], Priti Kumari[1], Nicholas C. Palmateer[1], Shaikh B.A. Iqbal[1], Lindsay Fry[3,4], Vishvanath M. Nene[5], Claudia Daubenberger[6], Richard P. Bishop[3], Joana C. Silva[1,7*]

Affiliations:

[1]Institute for Genome Sciences, University of Maryland School of Medicine, Baltimore, MD, USA

[2]Biosciences eastern and central Africa-International Livestock Research Institute, Nairobi, Kenya

[3]Animal Disease Research Unit, Agricultural Research Service, USDA, Pullman, WA 99164-7030, USA

[4]Department of Veterinary Microbiology & Pathology, Washington State University Pullman, WA 99164-7040, USA

[5]International Livestock Research Institute, Nairobi, Kenya

[6]Swiss Tropical and Public Health Institute, Basel, Switzerland & University of Basel, Basel, Switzerland

[7]Department of Microbiology and Immunology, University of Maryland School of Medicine, Baltimore, MD, USA

[*]Corresponding author

Abstract (<350 words)

Background: Genome annotation remains a significant challenge because of limitations in the quality and quantity of the data being used to inform the location and function of protein-coding genes and, when RNA data are used, the underlying biological complexity of the processes involved in gene expression. However, comprehensive and descriptive genome annotations are valuable resources for answering biological research questions and discovering novel chemotherapeutic targets for disease treatment.

Results: Here, we apply our recently published RNAseq dataset derived from the schizont life-cycle stage of the apicomplexan parasite *Theileria parva*, which causes a devastating livestock disease in sub-Saharan Africa, to update structural and functional annotations across the entire nuclear genome.

Conclusions: The process of re-annotation led to novel insights into the organization and expression profiles of protein-coding sequences in this parasite, and uncovered a minimal N-glycosylation pathway that changes our current understanding of the evolution of this post-translation modification in apicomplexan parasites.

Key Words: *Theileria*, East coast fever, Genome, Re-annotation, N-glycosylation

Background

East Coast fever (ECF) in eastern, central, and southern Africa causes an estimated loss of over 1 million heads of cattle yearly, with an annual economic loss that surpasses $300 million USD, impacting mainly smallholder farmers [1]. Cattle are the most valuable possession of smallholder farmers in this region, as they are a source of

milk, meat and hides, provide manure and traction in mixed crop-livestock systems, and revenue derived from livestock pays for school fees and dowries [2, 3]. ECF is a tick-transmitted disease caused by the apicomplexan parasite *Theileria parva*. Lymphocytes infected with *T. parva* proliferate in the regional lymph node draining the tick bite site, and then metastasize into various lymphoid and non-lymphoid organs, and induce a severe inflammatory reaction that leads to respiratory failure and death of susceptible cattle, which typically die within three to four weeks of infection [4-7]. *T. parva* control is vital to food security in this region of the world, which is plagued by a range of other infectious diseases of humans and their livestock.

Efficacious and affordable chemotherapeutics and vaccines are essential tools in the effective control of infectious disease agents [8, 9]. A reliable structural annotation of the genome, consisting at minimum of the correct location of all protein-coding sequences (CDSs), enables the identification, prioritization and experimental screening of potential vaccine and drug targets [10-12]. The accurate identification of the complete proteome can greatly enhance microbiological studies, and reveals metabolic processes unique to pathogens [13]. In turn, a better understanding of the biology of *T. parva* transmission, colonization and pathogenesis may ultimately reveal novel targets for pathogen control [14]. Currently, much like for other apicomplexan parasites [15, 16], knowledge on the functional role of genomic sequences outside of *T. parva* CDSs is sparse, and many gene models containing only CDSs are supported by little or no experimental evidence. RNAseq data, generated through deep sequencing of cDNA using next generation sequencing technologies, can provide an extraordinary level of insight into gene structure and regulation [12, 17]. Here, we used the first high-coverage

RNAseq data for this species [18] to improve existing gene models through the identification of start and stop codons, primary intron splice sites and untranslated regions (UTRs). This new gene model annotation brought to light several new insights into gene expression in this gene-dense eukaryote, and led to the discovery of several new prospective chemotherapeutic targets for treating ECF.

Results

The annotation of the Theileria parva *genome is significantly improved, revealing a higher gene density than previously thought*

The nuclear genome of the reference *T. parva* Muguga isolate consists of four linear chromosomes which are currently assembled into eight contigs (Supplementary Table S1, Additional File 1): chromosomes 1 and 2 are assembled into a single contig each, chromosome 3 is in four contigs and chromosome 4 in two [19]. The new genome annotation was based on this assembly and on extensive RNAseq data (Supplementary Figure S1, Additional File 1). We performed a comprehensive revision of the entire *T. parva* genome annotation, including automated structural annotation and a double-pass manual curation of each locus (see Methods).

The re-annotation process resulted in the discovery of 128 new genes, 274 adjacent gene models were merged, 157 gene models were split, and 38 genes were replaced by new genes encoded in the reverse orientation (Figure 1). In addition, exons boundaries have been corrected in over a thousand genes. Overall, 83% of all nuclear genes in the original annotation were altered in some way, with changes made on every

92 contig. This resulted in significant alterations to the predicted proteome, with 53% of the
93 nuclear proteins in the original annotation having altered amino acid sequences in the
94 new annotation, a remarkable ~50 bp increase in average CDSs length, a reduction of the
95 average length of intergenic regions by close to 100 bp and the assignment of an
96 additional 200,000 base pairs (or 2.4% of the genome), previously classified as intergenic
97 or intronic sequences, to the proteome. This results in a genome that is denser than
98 previously thought, with an overall increase in the coding fraction of the genome from
99 68% to 71%, more closely resembling *T. annulata* Ankara, which has a coding fraction of
100 72.9% (Supplementary Table S2, Additional File 1). In fact, *T. parva* has the densest
101 genome out of the indicated genomes investigated, with one protein-coding gene every
102 ~2100 bp (Supplementary Table S2, Additional File 1).
103 Several lines of evidence suggest that this annotation represents a very significant
104 improvement of the *T. parva* proteome relative to the original annotation. First, there was
105 an increase in the proportion of proteins with at least one PFAM domain in the new
106 proteome compared to the original proteome, implying that the new annotation captures
107 functional elements that were previously missed (Figure 2a). Given the close
108 evolutionary relationship and near complete synteny between *T. parva* and *T. annulata*
109 [20], their respective proteomes are expected to be very similar. Indeed, a comparison of
110 the two predicted proteomes results in 52 additional reciprocal best hits and protein
111 length differences between orthologs in *T. parva* and *T. annulata* also decreased
112 significantly (Figure 2b). It is likely that some of the most significant differences between
113 the *T. parva* and *T. annulata* proteomes, in particular the 25% fewer protein-coding genes
114 and much longer CDSs in the latter, represent annotation errors in the *T. annulata*

genome that will be corrected upon revision with more recently accumulated evidence. The total number of non-canonical splice sites in the genome increased from 0.15% to 0.36% of all introns, but the sequence diversity of non-canonical splice sites decreased from eight non-canonical splice donor and acceptor site combinations to only a single splice site pair – GC/AG donor and acceptor dinucleotides, recognized by the U2-type spliceosome [21] (Figure 2c). The new annotation is also considerably more consistent with the RNAseq data, with a larger number of introns, a higher proportion of which is supported by at least one RNAseq read (Figure 2d). A total of 118 introns from the original genome annotation have been removed, due to contradicting RNAseq evidence.

The tremendous power of RNAseq to inform on gene and isoform structure in this species revealed a significant amount of transcriptome diversity and complexity. First, the proportion of loci, defined here as a continuous genomic region encoding the length of a CDS, intervening introns, and flanking UTRs, that appear to overlap an adjacent locus increased from 2% to 10% in the new annotation. In many of these instances, read coverage, coding potential, and other evidence support the presence of adjacent genes with overlapping UTRs. In 125 cases, the overlap includes not only UTRs but also CDSs. Secondly, there are many instances of overlapping loci in which the respective CDSs are encoded in the same strand; in these cases, no UTRs were defined in the intervening intergenic region, since their exact boundaries could not be determined. Finally, during manual curation, we observed many instances of potential alternative splicing, the clearest of which were the cases of well-supported introns where RNAseq coverage was nevertheless significantly higher than zero. In these cases, only the most prevalent isoform was annotated (Figure 1f). Finally, despite its power, RNAseq evidence is not

sufficient to resolve the structure of all loci; when the evidence did not clearly favor one gene model over another, the gene model in the original annotation was maintained by default. Interestingly, the vast majority of the genes appear to have only one or, sometimes, two most prevalent isoforms, as has been proposed for *Plasmodium* [22], although this was not defined quantitatively here. The median length of the annotated mRNA reported here is ~1,500 bp, and the maximum length >15,000 bp (Supplementary Figure S2, Additional File 1).

Most genes are transcribed during the schizont stage of the Theileria parva *life-cycle, and antisense transcription is widespread*

We sequenced cDNA generated from polyA-enriched total RNA collected from a *T. parva*-infected, schizont-transformed bovine cell line (see Methods section). A total of $8.3x10^7$ paired-end reads were obtained with an Illumina HiSeq 2000 platform, 70.04% of which mapped to the *T. parva* reference genome (Supplementary Table S1, Additional File 1). RNAseq provided a complete and quantitative view of transcription revealing that most of the genome of this parasite is transcribed during the schizont stage of its life cycle (Supplementary Figures S1, S3, Additional File 1). We found that 4011 of all 4054 (98%) predicted protein-coding parasite genes are transcribed at the schizont stage, and 12,172 of all 12,296 introns are supported by RNAseq reads (Figure 2d). We found evidence of expression for almost all of the known humoral and cellular immunity antigens (Supplementary Table S3, Additional File 1). In fact, Tp9, one of those antigens, is among the 15 most highly expressed genes in our dataset (Supplementary Table S4,

Additional File 1). Interestingly, its ortholog in *T. annulata* has been hypothesized to contribute to schizont-induced host cell transformation [23].

As has recently been suggested from *in silico* analyses [18], transcription in *T. parva* occurs from diverse kinds of promoters, with many instances of adjacent loci overlapping on the same or opposite strands. In fact, of the 4,085 predicted protein-coding nuclear genes, only 74 had an estimated reads per kilobase of transcript per million reads (RPKM) of zero and an additional 154 had RPKM<1. Interestingly, of the 74 genes with an RPKM of zero, most are hypothetical, with no predicted functional annotation, and without any high-confidence orthologs (Supplementary Table S5, Additional File 1). Since tRNAs are not polyadenylated, they were not found in our RNAseq dataset (Materials and Methods). Annotated protein-coding genes lacking RNAseq evidence are mostly orthologs of *Plasmodium falciparum* apicoplast proteins with mid blood stage expression [24, 25], *T. parva* repeat (*Tpr*) family proteins, or DUF529 domain-containing proteins (Supplementary Table S5, Additional File 1). These data are consistent with a study published in 2005, which used MPSS to estimate expression levels of *T. parva* genes in the schizont stage of the parasite [26], as well as a more recent study comparing gene expression between the schizont and the sporozoite/sporoblast stages [27]. The expression levels in the sense strand for each gene, as quantified by RPKM, when log-transformed, followed a unimodal distribution similar to a normal distribution (Figure 3a).

T. parva *multi-gene families show variable expression levels*

Large gene families are known to play a role in the pathogenesis of protozoan infections, perhaps the most well-known being the *var* gene family in *P. falciparum*. These genes encode proteins that are essential for the sequestration of infected red blood cells, a critical biological feature determining severe malaria pathology of *P. falciparum* [28]. Using the OrthoMCL algorithm as described previously [19], we clustered paralogs in this genome, identifying changes in the size of several of the largest *T. parva* gene families (Supplementary Table S6, Additional File 1), and finding variable patterns in their levels of expression (Supplementary Figure S4, Additional File 1). The roles of most of these gene families are not known. For example, the *Tpr* (*T. parva* repeat) gene family has been suggested to be rapidly evolving and expressed as protein in the piroplasm stages [19]. This is consistent with our findings, which show *Tpr* genes not to be highly expressed in the schizont (Supplementary Figure S4, Additional File 1) or the sporoblast (Supplementary Figure S5, Additional File 1) stages [27, 29]. Interestingly, in that same dataset, we find a significant up-regulation of subtelomeric variable secreted protein gene (SVSP) family genes in the sporozoite stages relative to both the sporoblast and schizont stages, suggesting that they may be important for invasion or the establishment of infection in the vertebrate host (Supplementary Figure S5, Additional File 1) [30].

This new *T. parva* genome annotation not only improved our resolution of the gene models of multi-gene family members and other transformation factors (Supplementary Figure S6, Additional File 1) [31], but also uncovered 128 genes that were not present in the original annotation.

204

205 *A mechanism of core N-glycosylation is now predicted in* T. parva

206 Among the 128 newly identified genes, one was annotated as a potential Alg14
207 ortholog, an important part of a glycosyltransferase complex in many organisms that add
208 a N-acetylglucosamine (GlcNAc) to the N-glycan precursor. N-glycosylation is an
209 important type of protein post-translation modification, during which a sugar is linked to
210 the nitrogen of specific amino acid residues, a process that occurs in the membrane of the
211 endoplasmic reticulum and is critical for both the structure and function of many
212 eukaryotic proteins. N-glycosylation is a ubiquitous protein modification process, but the
213 glycans being transferred differ among the domains of life [32]. However, in
214 apicomplexan parasites that infect red blood cells, there appears to be a selection against
215 long N-glycan chains [33]. *Theileria* parasites were previously believed to not add N-
216 acetylglucosamine to their glycan precursors, since sequence similarity searches did not
217 identify the necessary enzymes. While this previous study did not discover any Alg
218 enzymes, we find that *T. parva* has Alg7 (*Tp*Alg7; TpMuguga_01g00118), Alg13
219 (*Tp*Alg13; TpMuguga_02g00515), and Alg14 (*Tp*Alg14; TpMuguga_01g02045)
220 homologs, which show differential mRNA-level expression between the sporozoite and
221 schizont life cycle stages (Supplementary Figure S7, Additional File 1). In fact, the
222 structure of each of these *Theileria* proteins can be predicted *ab initio* with high
223 confidence (Supplementary Table S7, Additional File 1) and have predicted secondary
224 structural characteristics very similar to their homologs in *Saccharomyces cerevisiae*
225 (Figure 4a). However, the structure of the *Tp*Alg7-encoding locus was altered as a result
226 of the re-annotation effort and *Tp*Alg14 is the product of a newly identified gene, which

might have prevented the original identification of the pathway. Therefore, *Theileria* parasites likely have a minimal N-glycosylation system. Interestingly, we can find Alg14 orthologs by blastp search in *T. orientalis* (TOT_010000184), *T. equi* (BEWA_032670), but not in *T. annulata*. Using the adjacent gene, EngB, as a marker, a look at the *T. annulata* genomic region that is syntenic to *Tp*Alg14 revealed that *T. annulata* has a hypothetical gene annotated on the opposite strand (Figure 4b), which could be an incorrect annotation. A tblastn search of the *T. annulata* genome using *Tp*Alg14 led to the discovery of a nucleotide sequence which translated results in an alignment with E-value of $7x10^{-15}$ and 70% identity over the length of the protein, suggesting the existence of an *T. annulata* Alg14 ortholog (*Ta*Alg14). In fact, the gene model that was at the *Tp*Alg14 locus in the original annotation, TP01_0196, was likely a result of an incorrect annotation transfer from *T. annulata* (or vice-versa), since TP01_0196 shared 52% identity with the gene annotated on the opposite strand at the putative *Ta*Alg14 locus (E-value $4x10^{-131}$). Since previous studies have used *T. annulata* as a model *Theileria* parasite, this could be the reason that N-glycosylation was not discovered in this parasite genus.

While the presence of N-glycans in *Plasmodium* parasite proteins was initially controversial [34], more recent work provided evidence of short N-glycans on the exterior of *P. falciparum* schizonts and trophozoites [35]. As a key difference, *Plasmodium* parasites have a clear ortholog of the oligosaccharyl transferase STT3 (EC 2.4.99.18, PF3D7_1116600 in *P. falciparum* 3D7), which catalyzes the transfer of GlcNAc and $GlcNAc_2$ to asparagine residues in nascent proteins, and recent work has identified several other proteins in this protein complex in *Plasmodium* genomes [34]. No such ortholog was found in *T. parva* Muguga or *T. annulata* Ankara by blastp or tblastn searches with the *Plasmodium* protein. Since there are STT3 orthologs in *T. equi* and *T. haneyi* (Figure

4c), as well as *Cytauxoon felis*, it appears that the absence of STT3 in *T. parva* and *T. annulata* represents evolutionary loss of STT3 orthologs in this lineage. This means that while lipid precursor N-glycosylation does likely occur at the ER in these two species, the canonical mechanism of N-glycan precursor transfer to proteins is apparently absent.

Discussion

The re-annotation of the *T. parva* genome has resulted in significant improvement to the accuracy of gene models, showing that this genome is even more gene-dense than previously thought, with the addition of 2.4% of the genome to CDSs as well as the discovery of additional overlapping genes. Multi-gene families appear to have played a prominent role in the evolution of the lineage leading to *T. parva* and *T. annulata* [36], implying a role for these genes in host-pathogen interactions. These genes have diversified and/or expanded in copy number, possibly as an adaptation to a particular niche, since the high density of the genome is strongly suggestive of selection against non-functional DNA. We now have a clearer picture of the structure, copy number, and relative expression level of these genes. In addition, a recently generated sporozoite and sporoblast datasets opens up new opportunities to study differential gene expression throughout other stages of the parasite life cycle [27].

The model of transcription that emerges from these recent studies is one of ubiquitous transcription of most genes in the schizont stage, but with a wide range of expression levels [18, 26, 27], suggesting that there are likely important *cis* regulatory motifs that control the level of expression or mRNA stability [18, 37]. Transcription can also arise from potential bidirectional and cryptic promoters with highly prevalent antisense transcription. It remains to be determined if sense and anti-sense transcripts are

generated in the same or different cells in culture, an issue that may be addressed with single-cell RNAseq. Due to the short-read nature of our sequencing platform, we were only able to accurately annotate the most prevalent isoform of each gene. The sequencing of full-length transcripts, for example with Pacific Biosciences sequencing technology, would provide a more comprehensive description of the *T. parva* transcriptome, including alternatively spliced variants and the boundaries of overlapping transcripts.

In yeast and humans, antisense transcription, defined by the existence of non-coding RNA encoded on the DNA strand opposite to, and overlapping with, that encoding the mRNA, is rare compared to sense transcription [38]. In *T. parva*, however, antisense transcription is highly prevalent throughout the genome (Figure 3b), as has been found in *P. falciparum*, where antisense transcription is synthesized largely by RNA polymerase II [39, 40] and can alter the expression of multigene family members by regulating the packaging of these loci into chromatin [41]. Most of the antisense transcripts seem to completely overlap with their sense counterparts, although the functional relevance of this observation has yet to be determined.

The discovery of evidence that N-glycosylation may occur in *Theileria* parasites could open up novel treatment options against *Theileria* infections. N-glycosylation is thought to be important for *Toxoplasma gondii* invasion, growth, and motility [42-44]. While the results are somewhat confounded by a lack of inhibitor specificity, treatment with the N-glycosylation inhibitor tunicamycin results in parasites with abnormal endoplasmic reticulum, malformed nuclei, and impaired secretory organelles [45]. While once controversial due to differences in analytical methods, parasite life-cycle stages, and host contamination, *P. falciparum* is now thought to have N-glycosylated proteins,

297 although this is not as frequent a mechanism of protein modification as
298 glycosylphosphatidylinositol [46] . This work has been supported by bioinformatic
299 analyses, finding that *P. falciparum* contains (albeit few) glycosyltransferases [47]. Early
300 work using N-glycosylation inhibitors has shown strong *in vitro* growth inhibition of
301 *Plasmodium* asexual blood stages [48-52], but the function of N-glycosylation of
302 apicomplexan parasite proteins is a topic that requires further study. Importantly, the lack
303 of an STT3 ortholog in *T. parva*, if true, would suggest that protein-targeted N-
304 glycosylation does not occur in this parasite (as does in *Plasmodium*), and may only
305 occur on the ER and potentially the surface of the parasite. Even though cytoplasmic N-
306 glycosyltransferases have been found in bacteria, they have not been found in eukaryotes,
307 and their presence in *T. parva* seems unlikely. The absence of a N-glycan protein transfer
308 system is largely supported by genome-wide searches for the enrichment of N-glycan
309 acceptor sites in *T. annulata* [53]. While N-glycosylation is often touted as an 'essential'
310 protein modification in eukaryotes [54], the absence of an STT3 ortholog in some
311 *Theileria* species suggests that this process may be critical as a lipid, rather than protein,
312 modification. This does not diminish the potential relevance of N-glycosylation in these
313 parasites. Regardless of whether these short N-glycans provoke host immune responses
314 or play a homeostatic role in parasite protein folding, they could be important therapeutic
315 targets. Finally, given the possibility that glycans encode immunological 'self', 'non-self'
316 or 'damage' identities [55], it is tempting to speculate that the absence of proteinaceous
317 N-glycans in *Theileria* species could represent an evolutionary adaptation to immune
318 evasion in a parasite lineage that resides free in the host cytoplasmic environment.
319

Conclusions

This study emphasizes the critical interplay between genome annotations and our knowledge of pathogen biology. The significant improvement of the *T. parva* Muguga reference genome gene annotation will facilitate numerous studies of this parasite to come, and has already given better resolution to genome-wide patterns of gene transcription, including antisense transcription and transcription from multi-gene families. The better the resolution at which we understand gene structure and expression, the more accurately we can characterize and study gene function, novel druggable pathways suitable for interventions and, ultimately, the biology of the pathogen in its different host organisms. For example, the discovery of N-glycosylation precursors in some *Theileria* parasites in the absence of a protein transfer system opens up new questions about the role of lipid N-glycosylation precursors in eukaryote biology as well as the potential evolutionary reasons why protein N-glycosylation would be lost in this apicomplexan lineage.

Methods

1) RNA sequencing and genome annotation

An RNA sample was obtained from the reference *T. parva* isolate (Muguga) from the haploid schizont stage of the parasite life cycle, which proliferates in host lymphocytes. The extraction method included complement lysis of schizont-infected host lymphocytes, DNase digestion of contaminating host DNA and differential centrifugation to enrich for schizonts [26, 56]. PolyA-enriched RNA was sequenced using Illumina

sequencing technology, to produce strand-specific RNAseq data. RNAseq reads were aligned with TopHat and RPKM values calculated using an in-house Perl script.

2) Genome re-annotation

For the re-annotation of the *Theileria parva* genome, a number of evidence tracks were generated and loaded into the genome browser JBrowse [57] for manual curation using the WebApollo plugin [58]. RNAseq reads were aligned to the genome with TopHat [59], a splice-aware alignment tool (Supplementary Table S1, Additional File 1). These alignments were used to generate strand-specific read alignment coverage glyphs and XY plots for visualization in WebApollo. TopHat alignment also yields a file of all reported splice junctions using segmented mapping and coverage information, which is useful for curating intron splice sites. RNAseq reads were also assembled into transcripts using CuffLinks [60] and mapped to the genome with TopHat. We also generated two genome-dependent Trinity/PASA [61] transcriptome assemblies (one reference annotation-dependent and one independent of the reference annotation), as well as one completely *de novo* Trinity transcriptome assembly. A variety of other proteome data were aligned to the genome with AAT [62] and used as evidence tracks, including previously generated *Theileria annulata* mass spectrometry data [63], and all non-*Theileria* apicomplexan proteins from NCBI's RefSeq.

In order to assess gene prediction accuracy before the manual curation phase, a set of 342 high-confidence *T. parva* gene models were selected from the current reference annotation on the basis of two criteria: (1) RNAseq reads must cover each exon in the gene, (2) Trinity *de novo* assembled transcripts and read coverage must be concordant

with the presence or absence of any introns in the gene model. Out of these 342 genes, 50 were randomly selected as a validation set and the remaining 292 were used as a training gene set for gene prediction software. The exon distribution of the validation set closely resembles that of the training set (Supplementary Table S8, Additional File 1).

Multiple gene prediction software tools were used and then assessed by the accuracy with which they predict the validation set using an in-house script. These included: *i*) Augustus [64], using RNAseq reads, the *T. parva* training gene set, or no evidence; *ii*) Semi-HMM-based Nucleic Acid Parser (SNAP) [65] and Glimmer [66] were trained with the *T. parva* training set; *iii*) Fgenesh [67] used a pre-existing training set of *Plasmodium* genes from its website; *iv*) the *ab initio* predictor GeneMark-ES [68]. Finally, gene models were selected with the consensus predictor Evidence Modeler (EVM) [69], using 57, differently-weighted combinations of the other evidence, while maximizing prediction accuracy (Supplementary Figure S8, Additional File 1). Based on their performance in comparison with the validation set, only the top four EVM predictions were loaded as evidence tracks for use in manual curation (Supplementary Figure S9, Additional File 1). tRNA and rRNA predictions were generated using tRNAscan-SE [70] and RNAmmer [71] and loaded as evidence tracks, along with the original *T. parva* Muguga annotation (Supplementary Figure S10, Additional File 1). A genome-wide, double-pass, manual curation of all gene models was completed, weighing the RNAseq evidence over the evidence from alignments with homologs from other species and the gene prediction programs. The annotation assignments were allocated in 50 kb segments, with different annotators doing adjacent segments, as well as altering the annotator for the first and second pass in order to reduce annotator bias.

Functional annotation of the *T. parva* proteome consisted of HMM3 searches of the complete proteome against our custom HMM collection that includes TIGRFams [72], Pfams [73], as well as custom-built HMMs [74] and RAPSearch2 searches against UniRef100 (with a cutoff of $1x10^{-10}$). In addition, a TMHMM search which was used to assign "putative integral membrane protein" to proteins with 3 of more helical spans (assuming there were no other hits to the previous searches). These searches were synthesized using Attributor (https://github.com/jorvis/Attributor) to generate the final annotation based on the different evidence sources to assign gene product names, EC numbers, GO terms and gene symbols to genes, conservatively where possible.

3) Multi-gene family clustering

Genes were clustered with OrthoMCL, using an inflation value of 4 and a BLAST p-value cutoff of 10^{-5}, as previously done [19]. All individual conserved domain searches were done using NCBI's Conserved Domain Database version 3.11 [75] with 45,746 PSSMs, with an E-value threshold of 0.01 and a composition based statistics adjustment. HMM searches of the entire PFAM database were done using default settings.

List of abbreviations

ECF: East Coast fever

UTR: Untranslated Regions

CDS: Coding Sequence

RPKM: reads per kilobase million

Tpr: *T. parva* repeat family

411 SVSP: subtelomeric variable secreted protein

412 SNAP: Semi-HMM-based Nucleic Acid Parser

413

414 **Ethics approval and consent to participate**

415 Not applicable.

416

417 **Consent for publication**

418 Not applicable.

419

420 **Availability of data and materials**

421 The *T. parva* Muguga re-annotation is publicly available in GenBank and can be

422 visualized at the following online link (http://jbrowse.igs.umaryland.edu/t_parva/), as

423 well as under the NCBI BioProject PRJNA16138.

424

425 **Competing interests**

426 The authors declare that they have no competing interests.

427

428 **Funding**

429 This work was supported in part by an Immunity and Infection T32 training grant,

430 NIH/NIAID T32 AI007540-14, by the by the Bill and Melinda Gates Foundation

431 (OPP1078791), and by the United States Department of Agriculture, Agricultural

432 Research Service (USDA-ARS) through agreement #59-5348-4-001.

433

Authors' contributions

RP isolated *T. parva* schizont RNA for RNAseq using differential centrifugation and standard kits as described. JO, OOI, and PK built and maintained the JBrowse instance for manual curation using the WebApollo plugin, as well as the functional annotation pipeline. KT, JO, HTG, OOI, PK, and SBAI generated alignment tracks to assist the annotation. KT, HTG, OOI, NCP, SBAI, JCS completed manual re-annotation of the genome. KT performed all other analyses. JCS, RPB, CD, VMN, and LF conceived the study design. KT and JCS wrote the manuscript. All authors critically reviewed and approved the manuscript.

Acknowledgements

We would like to thank Donald P. Knowles for his kind and helpful feedback and support for this project.

Figures and Figure Legends

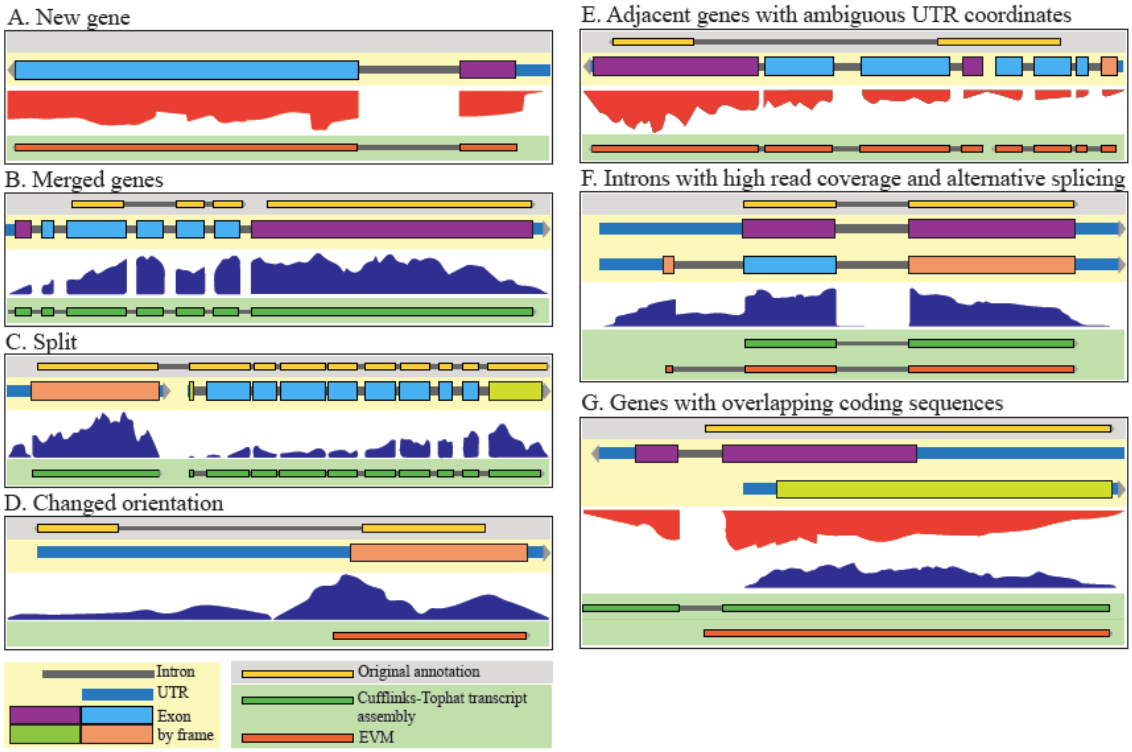

Figure 1. Manual gene model curation examples. Several tracks are shown: updated gene model (beige background), original (2005) gene annotation (grey background), RNAseq data (white background), transcript assembly (dark green, on green background), and EVM predictions (orange, on green background). (A) A new gene discovered on the basis of RNAseq data (TpMuguga_03g02005). (B) A case where two genes in the 2005 annotation merge in the new annotation on the basis of RNAseq read coverage (TpMuguga_04g02435). (C) A case where a gene in the 2005 annotation has been split into two genes in the new annotation (TpMuguga_04g02190 and TpMuguga_04g02185). (D) A case where a gene has been reversed in orientation on the basis of RNAseq data (TpMuguga_02g02095). (E) A case where overlapping genes led to ambiguity in UTR coordinates, and so the UTRs were not defined in this intergenic region (TpMuguga_01g00527 and TpMuguga_01g00528). (F) A case of a single gene

where alternative splicing exists (as seen by significant read coverage in at least one intronic region), but there is one most prevalent isoform (TpMuguga_03g00622). (G) A case of two genes that overlap by coding sequences. Coding exons are colored by reading frame (TpMuguga_05g00017 and TpMuguga_05g00018).

A

Species	Proteome Size (#)	% >= 1 PFAM hit	Year Published
***Theileria parva* Muguga (2019)**	**4055**	**61%**	**2019**
***Theileria parva* Muguga (2005)**	**4079**	**58%**	**2005**
Theileria annulata Ankara	3792	60%	2005
Theileria equi WA	5332	53%	2012
Theileria orientalis Shintoku	4002	59%	2012
Babesia bovis T2Bo	3703	63%	2007
Plasmodium vivax Sall	5393	62%	2008
Plasmodium falciparum 3D7	4555	61%	2002

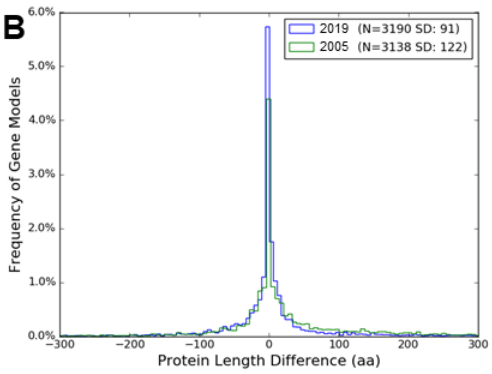

C

2005		2019	
Splice Sites	Frequency (#)	Splice Sites	Frequency (#)
GT...AG	10,406	GT...AG	12,445
GC...AG	5	GC...AG	45
TG...TA	4		
TG...AA	2		
AT...TG	1		
AA...TA	1		
GT...AA	1		
AT...TA	1		
AC...TA	1		
Total	10,422	Total	12,490

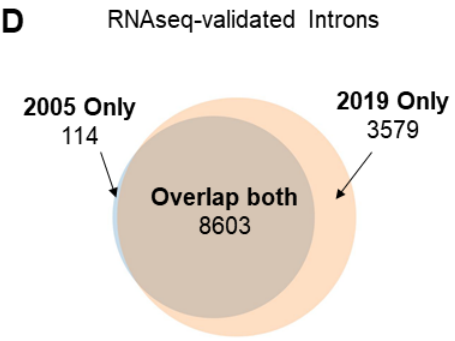

Figure 2. Comparative metrics of original and new *T. parva* annotations.

(A) The percentage of proteins with at least one PFAM domain found by Hidden Markov Model searches of the predicted proteomes of the new *T. parva* Muguga annotation was 2% higher than those in the 2005 annotation, implying that the new annotation captures functional elements that were previously missed. (B) The new *T. parva* Muguga annotation has more reciprocal best-hit orthologs (N) with *T. annulata* Ankara than the 2005 *T. parva* Muguga annotation. The variation in protein length (SD) between *T. parva* and *T. annulata* ortholog pairs is greatly reduced in the new relative to the original *T. parva* annotation. Only nuclear genes were used for this analysis. The x-axis was limited to the range -300 to +300 for easy visual interpretation. (C) The number of canonical GT/AG intron splice sites increased and the number of non-canonical intron splice site

combinations decreased in the new *T. parva* Muguga annotation compared to the 2005 annotation. (D) The number and proportion of introns validated by at least one RNAseq read increased in the new *T. parva* Muguga annotation compared to the 2005 annotation. These lines of evidence suggest that the new annotation is more accurate, and also considerably more consistent with the RNAseq data, as expected.

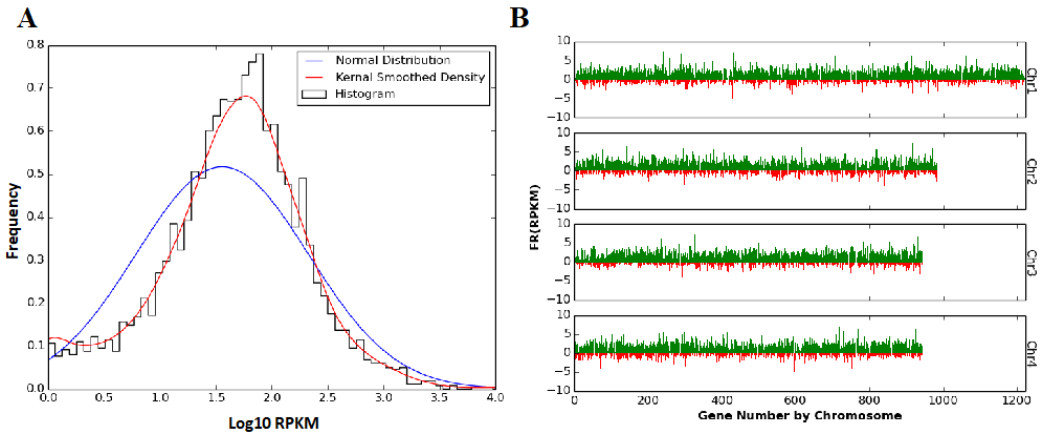

Figure 3. Distribution of RNAseq RPKM values for *T. parva* Muguga genes (A) A histogram of sense RPKM values after logarithmic transformation of the data. Frequencies on the y-axis correspond to probability density. The blue line shows a normal distribution around the same median, while the red line shows a more reliable fixed-width, Gaussian, kernel-smoothed estimate of the probability density. (B) The sense (green) and antisense (red) reads per kilobase transcript per million reads (RPKM) after fourth-root transformation of the data. Genes are sorted by position on the chromosome for all four nuclear chromosomes of *T. parva* Muguga.

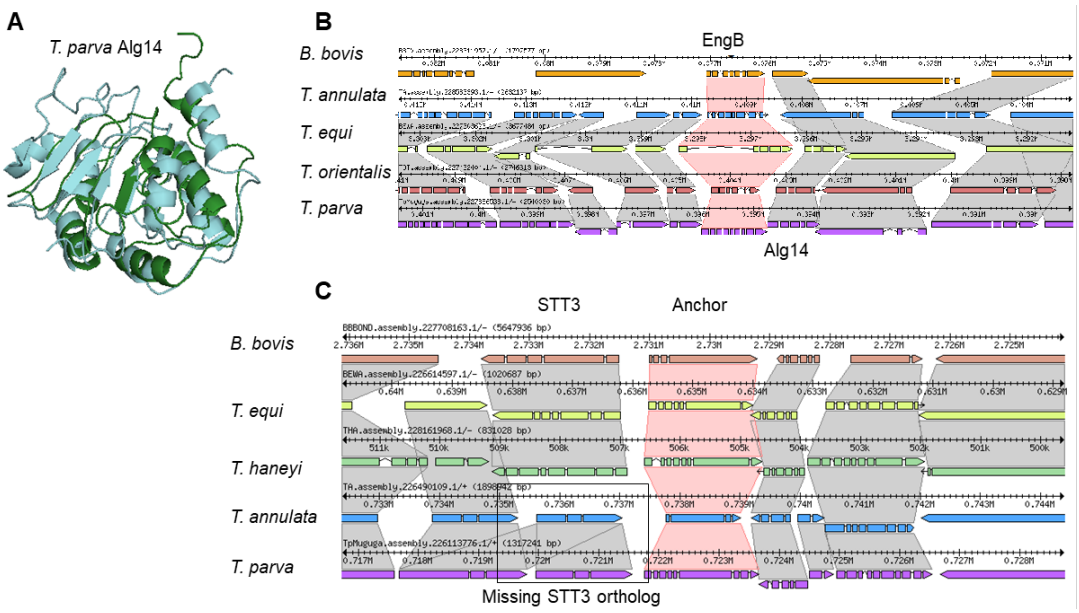

Figure 4. The uncovered *Theileria parva* Alg14 shows a similar predicted structure to the empirically determined *Saccharomyces cerevisiae* Alg14 protein structure, and is syntenic in multiple piroplasms. (A) A Phyre2 prediction of *T. parva* Alg14 (*Tp*Alg14; green; TpMuguga_01g02045) and the Protein Database (http://www.rcsb.org/) [76] nuclear magnetic resonance structure of *Saccharomyces cerevisiae* Alg14 (*Sc*Alg14; teal; PDB 2JZC) were aligned in MacPyMol (https://pymol.org/2/) [77]. (B) Shown are the syntenic regions around Alg14 orthologs (synteny in grey), using the adjacent gene EngB as an anchor (synteny in red) in the Sybil software package [78]. (C) Shown are the syntenic regions around STT3 orthologs (synteny in grey), using a *B. bovis* STT3-adjacent gene (BBOV_II000210) as an anchor (synteny in red) in the Sybil software package.

References

1. Spielman DJ: **XVI Public-Private Partnerships and Pro-Poor Livestock Research: The Search for an East Coast Fever Vaccine**, vol. 1. Washington, D.C.: The National Academies Press; 2009.
2. Herrero M, Thornton PK, Notenbaert AM, Wood S, Msangi S, Freeman HA, Bossio D, Dixon J, Peters M, van de Steeg J *et al*: **Smart investments in sustainable food production: revisiting mixed crop-livestock systems**. *Science* 2010, **327**(5967):822-825.
3. Nkedianye D, Radeny M, Kristjanson P, Herrero M: **Assessing returns to land and changing livelihood strategies in Kitengela**. In: *Staying Maasai? Livelihoods, conservation and development in East African Rangelands.* Edited by Homewood K, Kristjanson P, Chevenix Trench P. Dordrecht, The Nethelands: Springer; 2009: 115-150.
4. Baldwin CL, Black SJ, Brown WC, Conrad PA, Goddeeris BM, Kinuthia SW, Lalor PA, MacHugh ND, Morrison WI, Morzaria SP *et al*: **Bovine T cells, B cells, and null cells are transformed by the protozoan parasite Theileria parva**. *Infection and immunity* 1988, **56**(2):462-467.
5. Tindih HS, Geysen D, Goddeeris BM, Awino E, Dobbelaere DA, Naessens J: **A Theileria parva isolate of low virulence infects a subpopulation of lymphocytes**. *Infection and immunity* 2012, **80**(3):1267-1273.
6. Irvin AD, Mwamachi DM: **Clinical and diagnostic features of East Coast fever (Theileria parva) infection of cattle**. *The Veterinary record* 1983, **113**(9):192-198.

584 7. Fry LM, Schneider DA, Frevert CW, Nelson DD, Morrison WI, Knowles DP:
585 **East Coast Fever Caused by Theileria parva Is Characterized by**
586 **Macrophage Activation Associated with Vasculitis and Respiratory Failure**.
587 *PLoS One* 2016, **11**(5):e0156004.
588 8. Hotez PJ, Molyneux DH, Fenwick A, Kumaresan J, Sachs SE, Sachs JD, Savioli
589 L: **Control of neglected tropical diseases**. *The New England journal of medicine*
590 2007, **357**(10):1018-1027.
591 9. Reed SL, McKerrow JH: **Why Funding for Neglected Tropical Diseases**
592 **Should Be a Global Priority**. *Clin Infect Dis* 2018, **67**(3):323-326.
593 10. Sette A, Rappuoli R: **Reverse vaccinology: developing vaccines in the era of**
594 **genomics**. *Immunity* 2010, **33**(4):530-541.
595 11. Seib KL, Dougan G, Rappuoli R: **The key role of genomics in modern vaccine**
596 **and drug design for emerging infectious diseases**. *PLoS genetics* 2009,
597 **5**(10):e1000612.
598 12. Hotez PJ, Fenwick A, Ray SE, Hay SI, Molyneux DH: **"Rapid impact" 10 years**
599 **after: The first "decade" (2006-2016) of integrated neglected tropical disease**
600 **control**. *PLoS Negl Trop Dis* 2018, **12**(5):e0006137.
601 13. Chaudhary K, Roos DS: **Protozoan genomics for drug discovery**. *Nature*
602 *biotechnology* 2005, **23**(9):1089-1091.
603 14. Oberg AL, Kennedy RB, Li P, Ovsyannikova IG, Poland GA: **Systems biology**
604 **approaches to new vaccine development**. *Current opinion in immunology* 2011,
605 **23**(3):436-443.

15. Wakaguri H, Suzuki Y, Sasaki M, Sugano S, Watanabe J: **Inconsistencies of genome annotations in apicomplexan parasites revealed by 5'-end-one-pass and full-length sequences of oligo-capped cDNAs**. *BMC Genomics* 2009, **10**:312.

16. Yeoh LM, Lee VV, McFadden GI, Ralph SA: **Alternative Splicing in Apicomplexan Parasites**. *MBio* 2019, **10**(1).

17. Yandell M, Ence D: **A beginner's guide to eukaryotic genome annotation**. *Nature reviews Genetics* 2012, **13**(5):329-342.

18. Tretina K, Pelle R, Silva JC: **Cis regulatory motifs and antisense transcriptional control in the apicomplexan Theileria parva**. *BMC genomics* 2016, **17**(1):128.

19. Gardner MJ, Bishop R, Shah T, de Villiers EP, Carlton JM, Hall N, Ren Q, Paulsen IT, Pain A, Berriman M *et al*: **Genome sequence of Theileria parva, a bovine pathogen that transforms lymphocytes**. *Science* 2005, **309**(5731):134-137.

20. Pain A, Renauld H, Berriman M, Murphy L, Yeats CA, Weir W, Kerhornou A, Aslett M, Bishop R, Bouchier C *et al*: **Genome of the host-cell transforming parasite Theileria annulata compared with T. parva**. *Science* 2005, **309**(5731):131-133.

21. Collins L, Penny D: **Complex spliceosomal organization ancestral to extant eukaryotes**. *Molecular biology and evolution* 2005, **22**(4):1053-1066.

627 22. Russell K, Hasenkamp S, Emes R, Horrocks P: **Analysis of the spatial and**
628 **temporal arrangement of transcripts over intergenic regions in the human**
629 **malarial parasite Plasmodium falciparum**. *BMC genomics* 2013, **14**:267.
630 23. Unlu AH, Tajeri S, Bilgic HB, Eren H, Karagenc T, Langsley G: **The secreted**
631 **Theileria annulata Ta9 protein contributes to activation of the AP-1**
632 **transcription factor**. *PLoS One* 2018, **13**(5):e0196875.
633 24. Painter HJ, Carrasquilla M, Llinas M: **Capturing in vivo RNA transcriptional**
634 **dynamics from the malaria parasite Plasmodium falciparum**. *Genome*
635 *research* 2017.
636 25. Rovira-Graells N, Gupta AP, Planet E, Crowley VM, Mok S, Ribas de Pouplana
637 L, Preiser PR, Bozdech Z, Cortes A: **Transcriptional variation in the malaria**
638 **parasite Plasmodium falciparum**. *Genome research* 2012, **22**(5):925-938.
639 26. Bishop R, Shah T, Pelle R, Hoyle D, Pearson T, Haines L, Brass A, Hulme H,
640 Graham SP, Taracha EL *et al*: **Analysis of the transcriptome of the protozoan**
641 **Theileria parva using MPSS reveals that the majority of genes are**
642 **transcriptionally active in the schizont stage**. *Nucleic acids research* 2005,
643 **33**(17):5503-5511.
644 27. Tonui T, Corredor-Moreno P, Kanduma E, Njuguna J, Njahira MN, Nyanjom SG,
645 Silva JC, Djikeng A, Pelle R: **Transcriptomics reveal potential vaccine**
646 **antigens and a drastic increase of upregulated genes during Theileria parva**
647 **development from arthropod to bovine infective stages**. *PLoS One* 2018,
648 **13**(10):e0204047.

649 28. Deitsch KW, Dzikowski R: **Variant Gene Expression and Antigenic Variation**
650 **by Malaria Parasites**. *Annu Rev Microbiol* 2017, **71**:625-641.
651 29. Bishop R, Musoke A, Morzaria S, Sohanpal B, Gobright E: **Concerted evolution**
652 **at a multicopy locus in the protozoan parasite Theileria parva: extreme**
653 **divergence of potential protein-coding sequences**. *Mol Cell Biol* 1997,
654 **17**(3):1666-1673.
655 30. Schmuckli-Maurer J, Casanova C, Schmied S, Affentranger S, Parvanova I,
656 Kang'a S, Nene V, Katzer F, McKeever D, Muller J *et al*: **Expression analysis of**
657 **the Theileria parva subtelomere-encoded variable secreted protein gene**
658 **family**. *PLoS One* 2009, **4**(3):e4839.
659 31. Marsolier J, Perichon M, DeBarry JD, Villoutreix BO, Chluba J, Lopez T,
660 Garrido C, Zhou XZ, Lu KP, Fritsch L *et al*: **Theileria parasites secrete a prolyl**
661 **isomerase to maintain host leukocyte transformation**. *Nature* 2015,
662 **16**(520):378-382.
663 32. Schwarz F, Aebi M: **Mechanisms and principles of N-linked protein**
664 **glycosylation**. *Curr Opin Struct Biol* 2011, **21**(5):576-582.
665 33. Samuelson J, Robbins PW: **Effects of N-glycan precursor length diversity on**
666 **quality control of protein folding and on protein glycosylation**. *Semin Cell*
667 *Dev Biol* 2015, **41**:121-128.
668 34. Tamana S, Promponas VJ: **An updated view of the oligosaccharyltransferase**
669 **complex in Plasmodium**. *Glycobiology* 2019, **29**(5):385-396.
670 35. Bushkin GG, Ratner DM, Cui J, Banerjee S, Duraisingh MT, Jennings CV,
671 Dvorin JD, Gubbels MJ, Robertson SD, Steffen M *et al*: **Suggestive evidence for**

Darwinian Selection against asparagine-linked glycans of Plasmodium falciparum and Toxoplasma gondii. *Eukaryot Cell* 2010, **9**(2):228-241.

36. Reid AJ: **Large, rapidly evolving gene families are at the forefront of host-parasite interactions in Apicomplexa**. *Parasitology* 2015, **142 Suppl 1**:S57-70.

37. Pieszko M, Weir W, Goodhead I, Kinnaird J, Shiels B: **ApiAP2 Factors as Candidate Regulators of Stochastic Commitment to Merozoite Production in Theileria annulata**. *PLoS neglected tropical diseases* 2015, **9**(8):e0003933.

38. Ozsolak F, Kapranov P, Foissac S, Kim SW, Fishilevich E, Monaghan AP, John B, Milos PM: **Comprehensive polyadenylation site maps in yeast and human reveal pervasive alternative polyadenylation**. *Cell* 2010, **143**(6):1018-1029.

39. Militello KT, Patel V, Chessler AD, Fisher JK, Kasper JM, Gunasekera A, Wirth DF: **RNA polymerase II synthesizes antisense RNA in Plasmodium falciparum**. *RNA* 2005, **11**(4):365-370.

40. Lopez-Barragan MJ, Lemieux J, Quinones M, Williamson KC, Molina-Cruz A, Cui K, Barillas-Mury C, Zhao K, Su XZ: **Directional gene expression and antisense transcripts in sexual and asexual stages of Plasmodium falciparum**. *BMC Genomics* 2011, **12**:587.

41. Jing Q, Cao L, Zhang L, Cheng X, Gilbert N, Dai X, Sun M, Liang S, Jiang L: **Plasmodium falciparum var Gene Is Activated by Its Antisense Long Noncoding RNA**. *Front Microbiol* 2018, **9**:3117.

42. Fauquenoy S, Morelle W, Hovasse A, Bednarczyk A, Slomianny C, Schaeffer C, Van Dorsselaer A, Tomavo S: **Proteomics and glycomics analyses of N-**

glycosylated structures involved in Toxoplasma gondii--host cell interactions. *Mol Cell Proteomics* 2008, **7**(5):891-910.

43. Gas-Pascual E, Ichikawa HT, Sheikh MO, Serji MI, Deng B, Mandalasi M, Bandini G, Samuelson J, Wells L, West CM: **CRISPR/Cas9 and glycomics tools for Toxoplasma glycobiology**. *J Biol Chem* 2019, **294**(4):1104-1125.

44. Sidik SM, Huet D, Ganesan SM, Huynh MH, Wang T, Nasamu AS, Thiru P, Saeij JPJ, Carruthers VB, Niles JC *et al*: **A Genome-wide CRISPR Screen in Toxoplasma Identifies Essential Apicomplexan Genes**. *Cell* 2016, **166**(6):1423-1435 e1412.

45. Luk FC, Johnson TM, Beckers CJ: **N-linked glycosylation of proteins in the protozoan parasite Toxoplasma gondii**. *Molecular and biochemical parasitology* 2008, **157**(2):169-178.

46. Cova M, Rodrigues JA, Smith TK, Izquierdo L: **Sugar activation and glycosylation in Plasmodium**. *Malar J* 2015, **14**:427.

47. Samuelson J, Banerjee S, Magnelli P, Cui J, Kelleher DJ, Gilmore R, Robbins PW: **The diversity of dolichol-linked precursors to Asn-linked glycans likely results from secondary loss of sets of glycosyltransferases**. *Proceedings of the National Academy of Sciences of the United States of America* 2005, **102**(5):1548-1553.

48. Trigg PI, Hirst SI, Shakespeare PG, Tappenden L: **Labelling of membrane glycoprotein in erythrocytes infected with Plasmodium knowlesi**. *Bull World Health Organ* 1977, **55**(2-3):205-209.

716 49. Udeinya IJ, Van Dyke K: **Labelling of membrane glycoproteins of cultivated**
717 **Plasmodium falciparum**. *Bull World Health Organ* 1980, **58**(3):445-448.
718 50. Udeinya IJ, Van Dyke K: **Plasmodium falciparum: synthesis of glycoprotein**
719 **by cultured erythrocytic stages**. *Experimental parasitology* 1981, **52**(3):297-
720 302.
721 51. Udeinya IJ, Van Dyke K: **Concurrent inhibition by tunicamycin of**
722 **glycosylation and parasitemia in malarial parasites (Plasmodium falciparum)**
723 **cultured in human erythrocytes**. *Pharmacology* 1981, **23**(3):165-170.
724 52. Udeinya IJ, Van Dyke K: **2-Deoxyglucose: inhibition of parasitemia and of**
725 **glucosamine incorporation into glycosylated macromolecules, in malarial**
726 **parasites (Plasmodium falciparum)**. *Pharmacology* 1981, **23**(3):171-175.
727 53. Cui J, Smith T, Robbins PW, Samuelson J: **Darwinian selection for sites of Asn-**
728 **linked glycosylation in phylogenetically disparate eukaryotes and viruses**.
729 *Proc Natl Acad Sci U S A* 2009, **106**(32):13421-13426.
730 54. Lombard J: **The multiple evolutionary origins of the eukaryotic N-**
731 **glycosylation pathway**. *Biol Direct* 2016, **11**:36.
732 55. Maverakis E, Kim K, Shimoda M, Gershwin ME, Patel F, Wilken R,
733 Raychaudhuri S, Ruhaak LR, Lebrilla CB: **Glycans in the immune system and**
734 **The Altered Glycan Theory of Autoimmunity: a critical review**. *J Autoimmun*
735 2015, **57**:1-13.
736 56. Graham SP, Pelle R, Honda Y, Mwangi DM, Tonukari NJ, Yamage M, Glew EJ,
737 de Villiers EP, Shah T, Bishop R *et al*: **Theileria parva candidate vaccine**
738 **antigens recognized by immune bovine cytotoxic T lymphocytes**. *Proceedings*

of the National Academy of Sciences of the United States of America 2006, **103**(9):3286-3291.

57. Skinner ME, Uzilov AV, Stein LD, Mungall CJ, Holmes IH: **JBrowse: a next-generation genome browser**. *Genome research* 2009, **19**(9):1630-1638.

58. Lee E, Helt GA, Reese JT, Munoz-Torres MC, Childers CP, Buels RM, Stein L, Holmes IH, Elsik CG, Lewis SE: **Web Apollo: a web-based genomic annotation editing platform**. *Genome biology* 2013, **14**(8):R93.

59. Kim D, Pertea G, Trapnell C, Pimentel H, Kelley R, Salzberg SL: **TopHat2: accurate alignment of transcriptomes in the presence of insertions, deletions and gene fusions**. *Genome biology* 2013, **14**(4):R36.

60. Roberts A, Pimentel H, Trapnell C, Pachter L: **Identification of novel transcripts in annotated genomes using RNA-Seq**. *Bioinformatics* 2011, **27**(17):2325-2329.

61. Grabherr MG, Haas BJ, Yassour M, Levin JZ, Thompson DA, Amit I, Adiconis X, Fan L, Raychowdhury R, Zeng Q *et al*: **Full-length transcriptome assembly from RNA-Seq data without a reference genome**. *Nature biotechnology* 2011, **29**(7):644-652.

62. Huang X, Adams MD, Zhou H, Kerlavage AR: **A tool for analyzing and annotating genomic sequences**. *Genomics* 1997, **46**(1):37-45.

63. Witschi M, Xia D, Sanderson S, Baumgartner M, Wastling JM, Dobbelaere DA: **Proteomic analysis of the Theileria annulata schizont**. *International journal for parasitology* 2013, **43**(2):173-180.

64. Stanke M, Morgenstern B: **AUGUSTUS: a web server for gene prediction in eukaryotes that allows user-defined constraints**. *Nucleic Acids Res* 2005, **33**(Web Server issue):W465-467.

65. Korf I: **Gene finding in novel genomes**. *BMC bioinformatics* 2004, **5**:59.

66. Delcher AL, Bratke KA, Powers EC, Salzberg SL: **Identifying bacterial genes and endosymbiont DNA with Glimmer**. *Bioinformatics* 2007, **23**(6):673-679.

67. Solovyev V, Kosarev P, Seledsov I, Vorobyev D: **Automatic annotation of eukaryotic genes, pseudogenes and promoters**. *Genome biology* 2006, **7 Suppl 1**:S10 11-12.

68. Borodovsky M, Lomsadze A: **Eukaryotic gene prediction using GeneMark.hmm-E and GeneMark-ES**. *Current protocols in bioinformatics / editoral board, Andreas D Baxevanis [et al]* 2011, **Chapter 4**:Unit 4 6 1-10.

69. Haas BJ, Salzberg SL, Zhu W, Pertea M, Allen JE, Orvis J, White O, Buell CR, Wortman JR: **Automated eukaryotic gene structure annotation using EVidenceModeler and the Program to Assemble Spliced Alignments**. *Genome biology* 2008, **9**(1):R7.

70. Lowe TM, Eddy SR: **tRNAscan-SE: a program for improved detection of transfer RNA genes in genomic sequence**. *Nucleic acids research* 1997, **25**(5):955-964.

71. Lagesen K, Hallin P, Rodland EA, Staerfeldt HH, Rognes T, Ussery DW: **RNAmmer: consistent and rapid annotation of ribosomal RNA genes**. *Nucleic acids research* 2007, **35**(9):3100-3108.

783 72. Haft DH, Selengut JD, White O: **The TIGRFAMs database of protein families**.
784 *Nucleic acids research* 2003, **31**(1):371-373.
785 73. Finn RD, Bateman A, Clements J, Coggill P, Eberhardt RY, Eddy SR, Heger A,
786 Hetherington K, Holm L, Mistry J *et al*: **Pfam: the protein families database**.
787 *Nucleic acids research* 2014, **42**(Database issue):D222-230.
788 74. Li L, Stoeckert CJ, Jr., Roos DS: **OrthoMCL: identification of ortholog groups**
789 **for eukaryotic genomes**. *Genome research* 2003, **13**(9):2178-2189.
790 75. Marchler-Bauer A, Bo Y, Han L, He J, Lanczycki CJ, Lu S, Chitsaz F, Derbyshire
791 MK, Geer RC, Gonzales NR *et al*: **CDD/SPARCLE: functional classification of**
792 **proteins via subfamily domain architectures**. *Nucleic Acids Res* 2017,
793 **45**(D1):D200-D203.
794 76. Berman HM, Westbrook J, Feng Z, Gilliland G, Bhat TN, Weissig H, Shindyalov
795 IN, Bourne PE: **The Protein Data Bank**. *Nucleic Acids Res* 2000, **28**(1):235-242.
796 77. Janson G, Zhang C, Prado MG, Paiardini A: **PyMod 2.0: improvements in**
797 **protein sequence-structure analysis and homology modeling within PyMOL**.
798 *Bioinformatics* 2017, **33**(3):444-446.
799 78. Riley DR, Angiuoli SV, Crabtree J, Dunning Hotopp JC, Tettelin H: **Using Sybil**
800 **for interactive comparative genomics of microbes on the web**. *Bioinformatics*
801 2012, **28**(2):160-166.
802

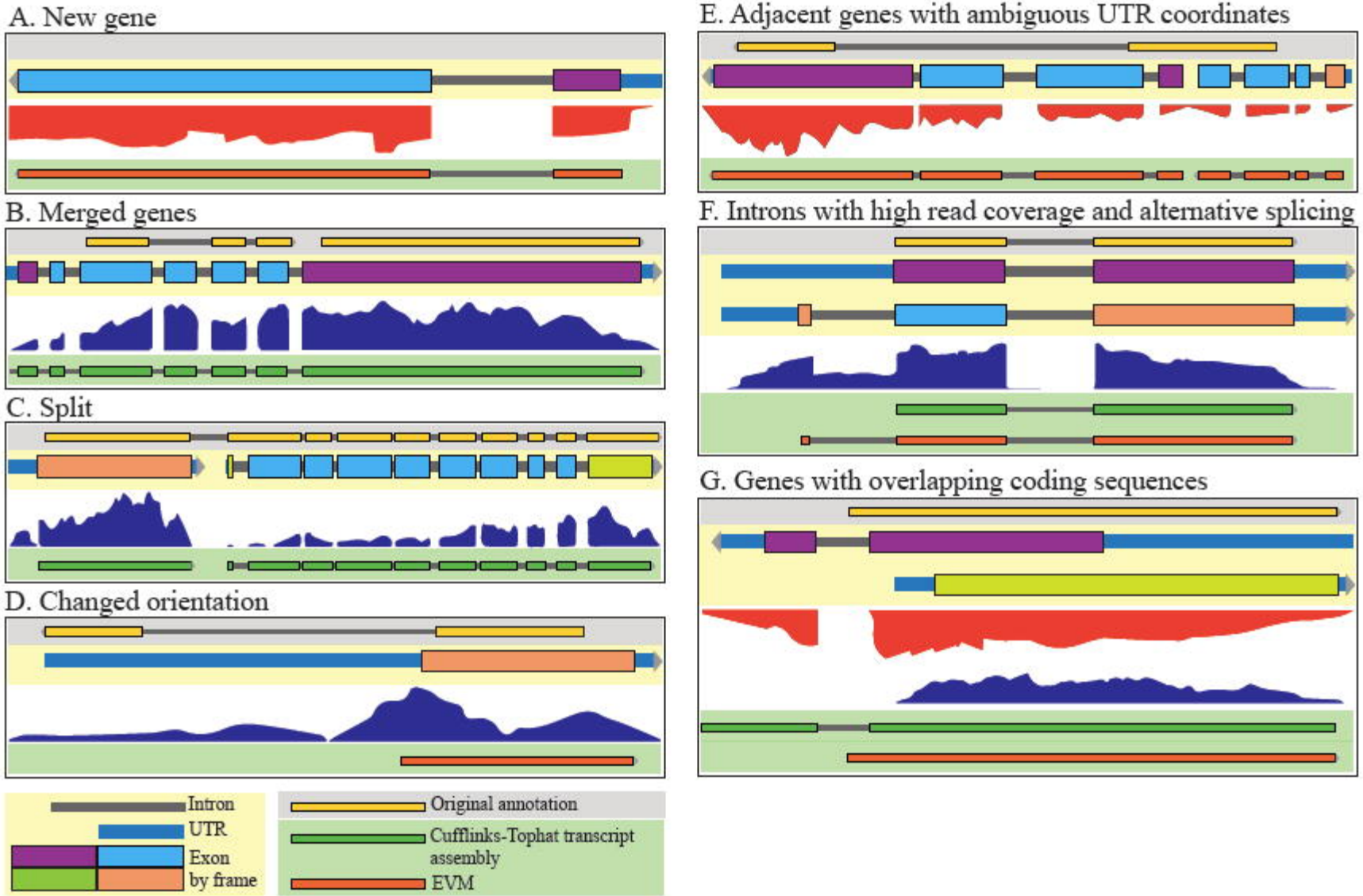
A. New gene
B. Merged genes
C. Split
D. Changed orientation
E. Adjacent genes with ambiguous UTR coordinates
F. Introns with high read coverage and alternative splicing
G. Genes with overlapping coding sequences
Intron
UTR
Exon
by frame
Original annotation
Cufflinks-Tophat transcript assembly
EVM

A

Species	Proteome Size (#)	% >= 1 PFAM hit	Year Published
Theileria parva Muguga (2019)	**4055**	**61%**	**2019**
Theileria parva Muguga (2005)	**4079**	**58%**	**2005**
Theileria annulata Ankara	3792	60%	2005
Theileria equi WA	5332	53%	2012
Theileria orientalis Shintoku	4002	59%	2012
Babesia bovis T2Bo	3703	63%	2007
Plasmodium vivax Sall	5393	62%	2008
Plasmodium falciparum 3D7	4555	61%	2002

B

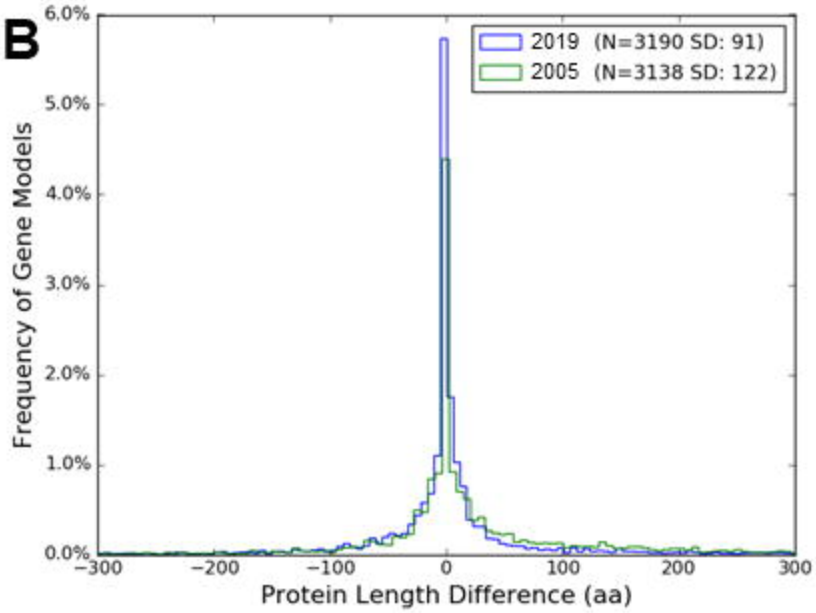

C

2005		2019	
Splice Sites	Frequency (#)	Splice Sites	Frequency (#)
GT...AG	10,406	GT...AG	12,445
GC...AG	5	GC...AG	45
TG...TA	4		
TG...AA	2		
AT...TG	1		
AA...TA	1		
GT...AA	1		
AT...TA	1		
AC...TA	1		
Total	10,422	Total	12,490

D

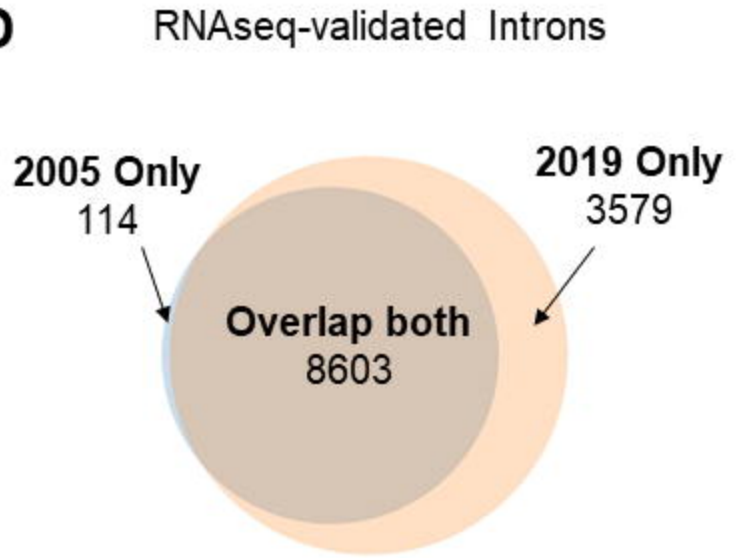

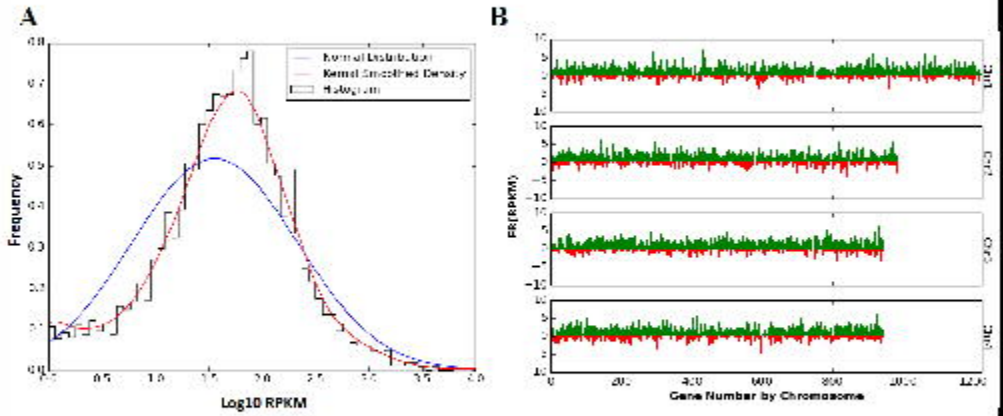
A
B
Frequency
Log10 RPKM
FR(RPKM)
Gene Number by Chromosome

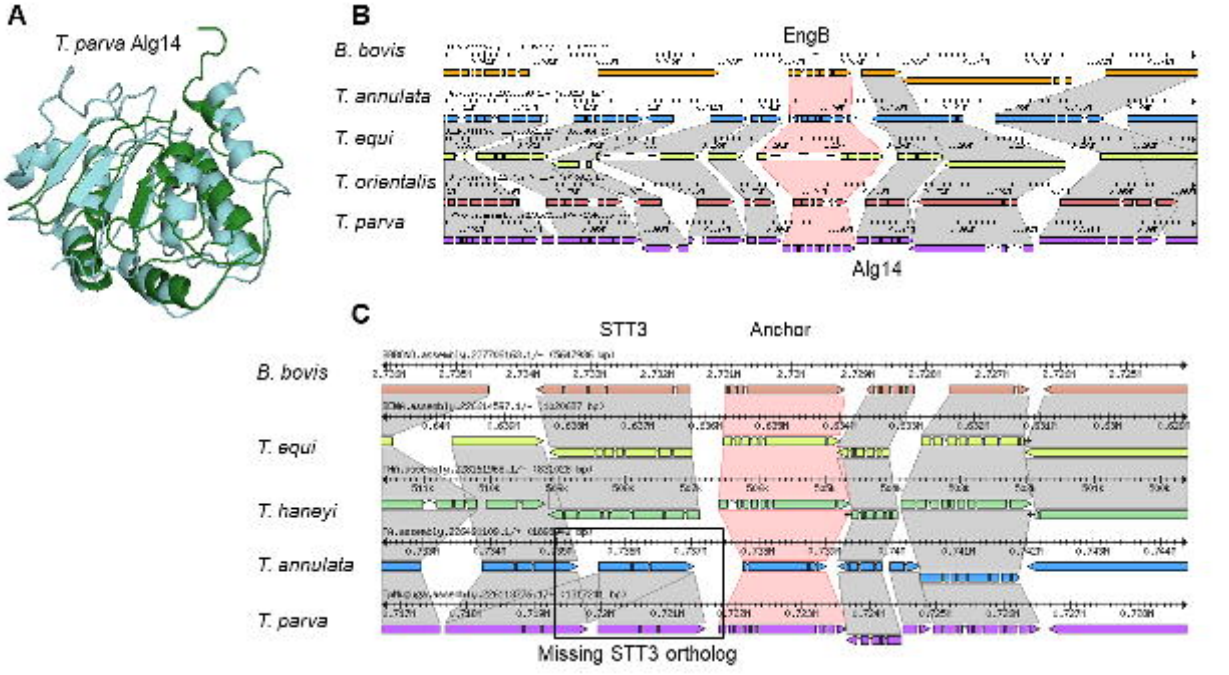
A
T. parva Alg14
B
EngB
B. bovis
T. annulata
T. equi
T. orientalis
T. parva
Alg14
C
STT3
Anchor
B. bovis
T. equi
T. haneyi
T. annulata
T. parva
Missing STT3 ortholog